Analysis, design and control of a resonant forward-flyback converter

Chao Quan[1], Yuchuan Geng[2], Qianhong Chen[2], Ming Xu[1], Julu Sun[1]

FSP-Powerland
Nanjing, China
chaoquan@fsp-powerland.com

College of Automation Engineering
Nanjing University of Aeronautics and Astronautics
Nanjing, China
chenqh@nuaa.edu.cn

***Abstract*—A resonant forward-flyback converter is proposed in this paper, in which the high efficiency resonant forward part delivers most of the power and the flyback part achieves tight regulation and magnetic resetting. Operating characteristics are analyzed in detail. As the key design parameters, this paper studies the influence of transformer's turns-ratios on component stress and power loss. A minimum duty cycle control strategy (D_{min}-fs) is proposed to guarantee ZCS of forward diode and valley switching. An experimental prototype of 400V input 48V output is built to verify the analysis. The prototype achieves a high efficiency of 96% at 120W output.**

Keywords—resonant forward; valley switching; Σ /sigma topology;

I. INTRODUCTION

High power density and high efficiency are two key elements of the DC/DC converter design. Due to the simple structure, high efficiency and low EMI characteristics, resonant converters such as LLC converters, resonant forward converters, have been widely used in server power supply, EV chargers and other applications[1]-[7]. A lot of researches have been made to further improve the performance of resonant converters. To reduce the volume of magnetics, the integration of the resonant inductor into the transformer has been introduced in LLC resonant converters [6]. Different integrated magnetic structures are proposed, investigated and compared so as to obtain higher efficiency and power density. Resonant forward converter is another promising resonant topology featuring compactness and zero current switching in the rectifier[7]. In [7], the quasi-ZVS turn-on and quasi-ZCS turn-off are both achieved and the high voltage stress in the traditional resonant forward converter is reduced by secondary diode-clamping. Some resonant converters have their optimum operation point with very high efficiency and load-independent output characteristics. Therefore, it is also an effective method to combine the converters operating at the optimum operation point with another converter together to achieve high efficiency and tight regulation simultaneously, i.e. Σ /sigma topology concept. In paper [4]-[5], the LLC DCX was combined with Input-series Output-parallel Flyback circuit with Σ/sigma topology concept. Most power was transmitted by LLC DCX and the Flyback was responsible for voltage regulation.

According to the concepts of Σ /sigma topology and magnetic integration, this paper proposes a resonant forward-flyback converter and analyzes its working principle. Both ZCS condition of forward diode and output voltage characteristic are derived in this paper. This paper conducts a study of the influence of transformer turns ratios on converter characteristics and gives the design basis of turns ratio from the view of efficiency optimization. Finally, this paper will present the control strategy of the system and carry out corresponding experiments to verify the theoretical analysis.

II. ANALYSIS OF THE PROPOSED RESONANT FORWARD-FLYBACK CONVERTER

A. Proposing of the resonant forward-flyback converter

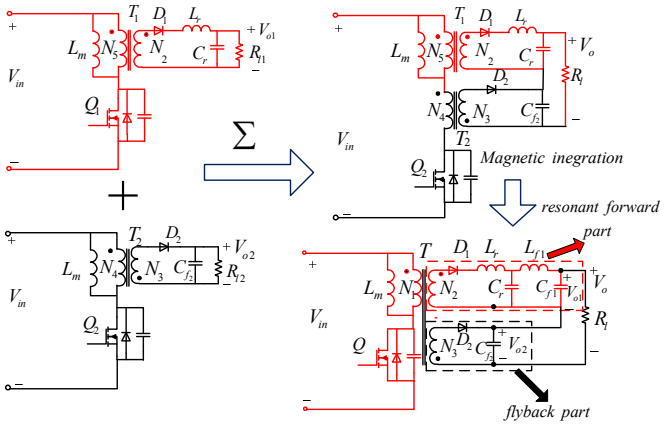

Fig.1 Resonant forward-flyback converter

Fig.1 shows the proposing of the resonant forward-flyback converter: Combining resonant forward converter with flyback converter using the concept of Σ/Sigma topology and applying magnetic integration, as shown in Fig.1, the resonant

forward-flyback converter can then be obtained. Where N_1, N_2, N_3, D_1, D_2, L_m, L_r, C_r and Q represent primary turns, resonant forward part turns, flyback part turns, forward diode, flyback diode, magnetizing inductor, leakage inductor, resonant capacitor and switch respectively.

B. *Characteristics analysis*

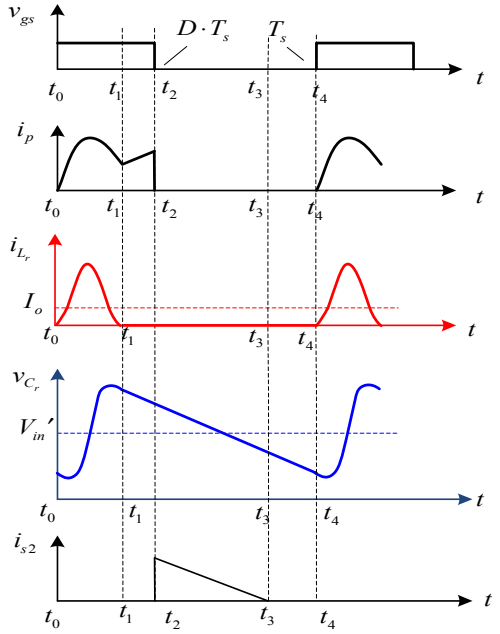

Fig.2(a)Key waveforms in FR-DCM mode

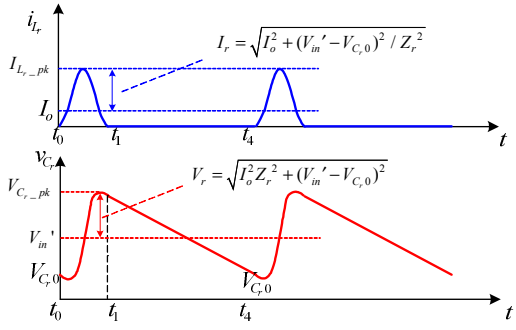

Fig.2(b) Key waveforms of the resonant forward part

There are several operation mode combinations for resonant forward part and flyback part. Forward part can operate in full resonant mode (FR) or partial resonant mode (PR), and flyback part can in DCM mode or CCM mode. In order to realize the ZCS for D_1 and valley switching for Q, the converter should work in FR- DCM mode which means forward part operates in FR and flyback part in DCM. Accordingly, only the key waveforms of the proposed converter in FR-DCM are given in Fig. 2(a).

To better understand the operating principle of the proposed converter, the operation mode of FR-DCM is briefly analyzed here.

Mode 1 [t_0-t_1]: When Q turns on at t_0, forward diode D_1 is conducting, leakage inductor L_r begins to resonant with resonant capacitor C_r and satisfied the resonant state equations (1) and (2), magnetizing current increases linearly, D_1 zero-current cuts off at t_1, the progress of resonance is ended and ZCS of D_1 is realized.

$$v_{Cr}(t) = V_{in}' - (V_{in}' - V_{C_r0})\cos\omega_r(t-t_0) - Z_r I_o \sin\omega_r(t-t_0) \quad (1)$$

$$i_{L_r}(t) = I_o - I_o\cos\omega_r(t-t_0) + (V_{in}' - V_{C_r0})\sin\omega_r(t-t_0)/Z_r \quad (2)$$

Where V_{cr0} is the initial voltage of C_r, and $V_{in'}$ is the induction voltage of the secondary winding when Q turns on.

Mode 2 [t_1-t_2]: The magnetizing current continues to increases linearly, the load energy is provided by C_r, C_r discharging linearly until Q turns off.

Mode 3 [t_2-t_3]: The resonant capacitor C_r continues to discharge, the flyback part begins to work, magnetizing inductor L_m demagnetizing and the transformer resets at t_3.

Mode 4 [t_3-t_4]: The magnetizing inductor L_m begins to resonant with the parasitic capacitor of Q and provides the condition for Q's valley switching.

Through the operation mode analysis in FR-DCM mode, we can get the conclusion that the proposed converter can both realize ZCS of D_1 and valley switching of Q, which is beneficial for efficiency improvement.

The expression of the output voltage of resonant forward and flyback can be found in the previous literature, as shown in (3) ~ (6).

FR: $$V_{o1\_FR} = V_{in}\frac{N_2}{N_1} \quad (3)$$

PR: $$V_{o1\_PR} = V_{in}\frac{N_2}{N_1} - V_{in}I_o\left[\frac{Z_r(1-\cos(\omega_r DT_s))}{\omega_r T_s \sin^2\theta} - \frac{(1-D)^2 Ts}{2C_r}\right] \quad (4)$$

DCM: $$V_{o2\_DCM} = \frac{V_{in}^2 D^2}{2L_m f_s I_o} \quad (5)$$

CCM: $$V_{o2\_CCM} = V_{in}\frac{N_3}{N_1}\frac{D}{1-D} \quad (6)$$

Then we can obtain the voltage gain of the proposed converter in different modes by getting the voltage gain of resonant forward part and flyback part respectively:

FR-CCM: $$V_o = V_{in}\cdot\left(\frac{N_2}{N_1} + \frac{N_3}{N_1}\cdot\frac{D}{1-D}\right) \quad (7)$$

FR-DCM: $$V_o = V_{in}\cdot\frac{N_2}{N_1} + \frac{V_{in}^2 D^2}{2L_m f_s I_o} \quad (8)$$

PR-DCM: $$V_o = V_{in}\cdot\frac{N_2}{N_1} + \frac{V_{in}^2 D^2}{2L_m f_s I_o} - I_o\left[\frac{Z_r(1-\cos(\omega_r DT_s))}{\omega_r T_s \sin^2\theta} - \frac{(1-D)^2 Ts}{2C_r}\right] \quad (9)$$

PR-CCM: $$V_o = V_{in}\cdot\left(\frac{N_2}{N_1} + \frac{N_3}{N_1}\cdot\frac{D}{1-D}\right) - I_o\left[\frac{Z_r(1-\cos(\omega_r DT_s))}{\omega_r T_s \sin^2\theta} - \frac{(1-D)^2 Ts}{2C_r}\right] \quad (10)$$

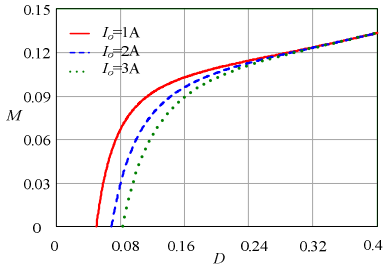

Fig.3 Fixed frequency voltage gain characteristic

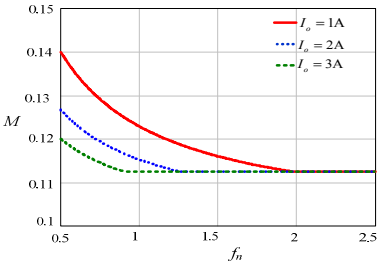

Fig.4 Variable frequency voltage gain characteristic

Fig.3 and Fig.4 illustrate the voltage gain M characteristics of the proposed converter where $M=V_o/V_{in}$. Under fixed frequency condition, the resonant forward part operates in the PR mode if D is relatively small, and the voltage gain M rises rapidly with the increase of D. The resonant forward part enters FR mode with constant gain as D continues to rise, then the output voltage is completely regulated by the flyback part. For variable frequency condition (with a constant D), once the converter enters FR-CCM mode at a certain frequency, the gain of the flyback is only related to D. The voltage gain M is no longer varies with the switching frequency in FR-CCM mode.

The characteristics analysis reveals that the proposed converter has the following advantages: (1) Compactness; (2) High efficiency due to the realizing of ZCS for D_1 and valley-switching for Q; (3) Most power is transmitted by resonant forward part which can improve the efficiency, and the flyback part realizes the voltage regulation and reset of transformer while delivering a small amount of power.

III. DESIGN AND CONTROL OF THE PROPOSED CONVERTER

A. Power allocation

The power allocation between forward part and flyback part is determined by their output voltage respectively. We can get the power allocation as follow:

$$\frac{P_{o1\_FR}}{P_{o2\_CCM}}=\frac{U_{o1\_FR}}{U_{o2\_CCM}}=\frac{K_1}{K_2}\cdot\frac{1-D}{D}$$
$$\text{or}\ \frac{P_{o1}}{P_{o2\_DCM}}=\frac{U_{o1\_FR}}{U_{o2\_DCM}}=K_1\cdot\frac{2L_mI_of_s}{V_{in}D^2} \quad (11)$$

where $K_1=N_2/N_1$, $K_2=N_3/N_1$. As shown in equation (11), different from the FR-CCM mode, the power allocation is determined by K_1, D, and f_s in FR-DCM mode.

B. Voltage Rating And Current Rating Analysis

As shown in Fig.2(b), the voltage rating and current rating of D_1 and Q is related to the resonant progress between L_r and C_r. the resonant impedance Z_r and resonance shift angle θ are defined respectively as:

$$\omega_r=1/\sqrt{L_rC_r},Z_r=\sqrt{L_r/C_r},\theta=\arctan\left[(I_oZ_r)/(V_{in}'-V_{C_r0})\right] \quad (13)$$

The I_r and V_r can be defined and simplified as:

$$I_r=\sqrt{I_o^2+(V_{in}'-V_{C_r0})^2/Z_r^2},V_r=\sqrt{I_o^2Z_r^2+(V_{in}'-V_{C_r0})^2} \quad (14)$$

$$I_r=I_o/\sin\theta,V_r=(I_oZ_r)/\sin\theta \quad (15)$$

Then, the expression of voltage and current rating of D_1 and Q can be simplified as follow:

$$V_{D1\_pk}=V_{in}\cdot K_1+\frac{I_oZ_r}{\tan\theta}+\frac{V_{in}^2D^2}{2L_mI_of_s}\cdot\frac{K_1}{K_2},$$
$$I_{D1\_pk}=I_o+\frac{I_o}{\sin\theta} \quad (16)$$

$$V_{Q\_pk}=V_{in}+V_{o2}/K_2,I_{Q\_pk}\approx(I_o+I_r)\cdot K_1 \quad (17)$$

D_1 reaches its peak voltage V_{D1_pk} when Q turn-off. The variation of V_{D1_pk} can be ignored from t_1 to t_2, So, V_{D1_pk} and I_{D1_pk} can be expressed as (16). Ignoring both the resonance between the leakage and the parasitic capacitance and exciting current, we can get the voltage stress and current stress of Q in (17), It can be found that the voltage stress of D_1 and Q can be reduced by increasing K_2.

C. Power Loss Analysis

When converter operates in DCM mode, we can calculate the turn-on loss P_{Q_on}, conduction loss P_{Q_cond} and turn-off loss P_{Q_off} use the following equations:

$$P_{Q\_on}=\frac{1}{2}C_{oss(on)}\cdot(V_{in}-V_{o2}/K_2)^2\cdot f_s \quad (18)$$

$$P_{Q\_cond}=I_{Q\_rms}^2\cdot R_{DS(on)}=K_1^2\cdot I_{D1\_rms}^2\cdot R_{DS(on)} \quad (19)$$

$$P_{Q\_off}=\frac{1}{2}(V_{in}+V_{o2}/K_2)\cdot I_{d\_off}\cdot(t_{chg}+t_f)\cdot f_s \quad (20)$$

Where $C_{oss(on)}$ is the equivalent output capacitance of Q, I_{d_off} is the current in Q when Q is switched off, t_{chg} is the junction capacitor charging time of the switch, and t_f is the time of the current down when the switch is switched off.

For winding loss:

$$P_{Cu\_fbk}=I_{D2\_rms}^2\cdot r_{fbk}\cdot N_3=I_{D2\_rms}^2\cdot r_{fbk}\cdot N_1\cdot K_2 \quad (21)$$

$$P_{Cu\_fwd}=I_{D1\_rms}^2\cdot r_{fwd}\cdot N_2=I_{D1\_rms}^2\cdot r_{fwd}\cdot N_1\cdot K_1 \quad (22)$$

$$P_{Cu\_p} = I_{p\_rms}^2 \cdot r_p \cdot N_1 = I_{D1\_rms}^2 \cdot r_p \cdot N_1 \cdot K_1^2 \quad (23)$$

Where P_{cu_fbk}, P_{cu_fwd}, P_{cu_p} represent the copper loss of flyback winding, forward winding and primary winding respectively. I_{D2_rms}, I_{D1_rms}, I_{p_rms}, r_{fbk}, r_{fwd}, r_p represent their RMS-currents and equivalent resistors. The resonant forward part delivers the most power which means that I_{D1_rms} is much larger then I_{D2_rms}, therefore the overall effect of increasing K_2 is to reduce the copper loss of the transformer. Through analysis the influence of turns ratio on efficiency, we can optimize the efficiency by using the method shown in Fig 5, and get the optimal turns ratio allocation by trade-off between the switching loss and the winding loss.

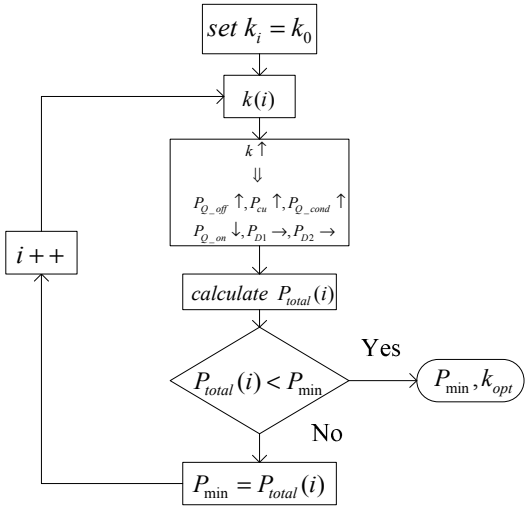

Fig.5 Efficiency optimization flow chart

D. Design and control of the converter

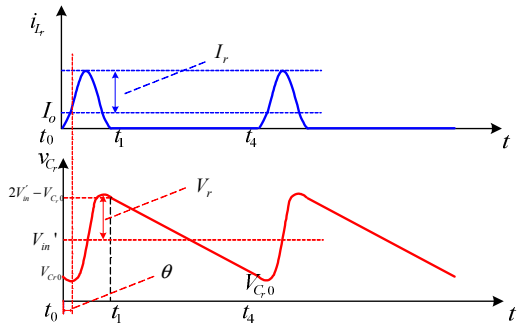

Fig.6 Key waveforms of the resonant forward part

According to the previous analysis, in order to realize both the ZCS of D_1 and valley switching of Q, the proposed converter has to operate in FR-DCM mode, so, derivation of the condition for FR-DCM is necessary :

I_{Lr} come to 0 at t_1:

$$I_r \sin(\omega_r t_1 - \theta) + I_o = 0 \quad (24)$$

During t_1 to t_4, C_r discharging linearly:

$$(2V_{in}' - V_{C_r0}) - V_{Cr0} = \frac{I_o}{C_r}(T_s - t_1) \quad (25)$$

Substituting equation(13), (15) and (25) into equation(24), then we can get the express of D_{min1} :

$$\cos(\omega_r t_1) - \frac{T_s - t_1}{2Z_r C_r}\sin(\omega_r t_1) - 1 = 0 \Rightarrow D_{\min 1} \quad (26)$$

Where D_{min1} stands for the critical D for realizing ZCS.

In order to ensure the converter operate in DCM mode, the duty cycle D and the switching frequency f_s also need to meet the constraint conditions:

$$I_o \le \frac{V_{in}}{2L_m f_s} D(1-D) \cdot \frac{N_1}{N_3} \quad (27)$$

So, we can get the condition for operating in DCM:

$$D_{\min 2} = \frac{1 - \sqrt{1 - \frac{8I_o f_s L_m}{V_{in}} \cdot \frac{N_3}{N_1}}}{2} \quad (28)$$

Where D_{min2} stands for the critical D for realizing valley switching.

A compound control method based on D_{min}-fs control, which ensures the achievement of ZCS and valley switching, is proposed in this paper, as showed in Fig 7. The condition of ZCS and valley switching is determined in (26) and (28). As shown in Fig 8, a constant on-time controller is used to guarantee ZCS and valley switching. Closed loop control is realized by frequency modulation.

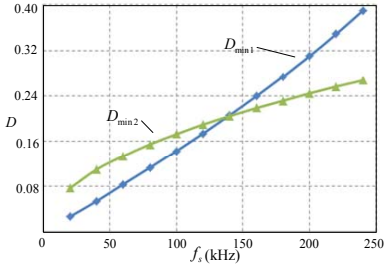

Fig.7 D_{min}-f_s control curve

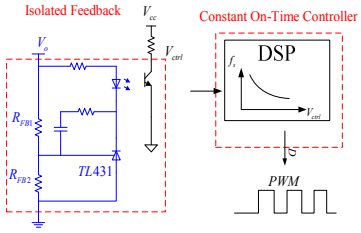

Fig.8 Control scheme

IV. EXPERIMENTAL VERIFICATION

A prototype with 400V input 48V /150W output is fabricated to verify the analysis. Two different turns ratios are

chosen for comparison as shown in Tab.3. Fig.10-Fig.12 illustrate the comparison experimental results.

TABLE I. TWO FEASIBLE TURNS RATIO FOR T

	N_1	N_2	N_3	K_1	K_2
Scheme A	44	4	2	1:11	1:22
Scheme B	36	4	1	1:9	1:36

A. *Realizing of ZCS and valley switching*

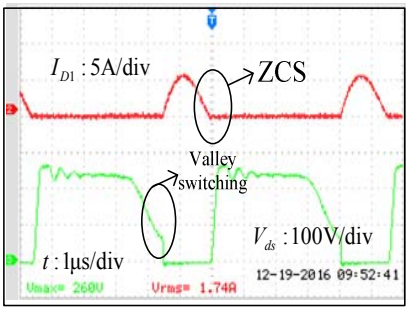

Fig.9 I_{D1}, V_{ds} in FR-DCM

Fig.9 shows the achieving of ZCS for the D_1 and valley switching for Q in FR-DCM.

B. *Comparison of scheme A and B*

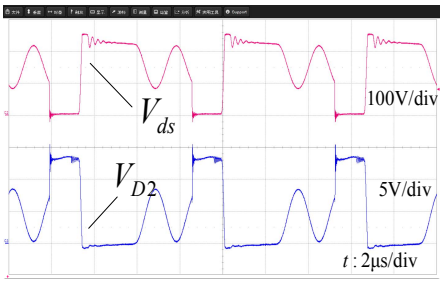

Fig.10 (a) V_{D2}, V_{ds} for scheme A

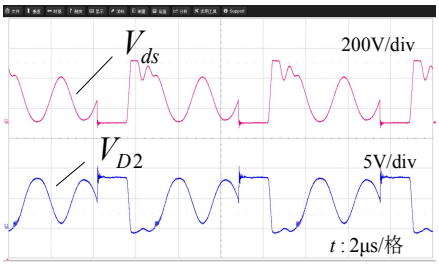

Fig.10 (b) V_{D2}, V_{ds} for scheme B

As shown in Fig.10(a) and Fig.10(b), when K_2 is reduced, the voltage stress of the flyback diode decreases while the voltage stress of the switch increases which agrees well with the theoretical analysis.

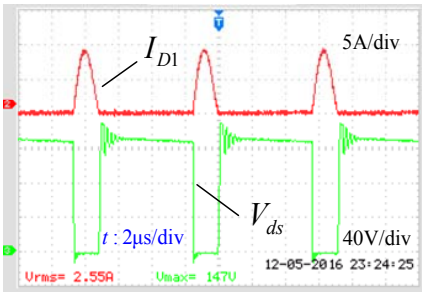

Fig.11 (a) I_{D1}, V_{ds} for scheme A

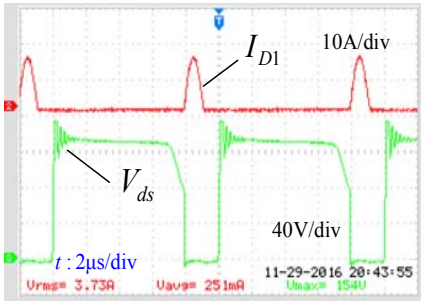

Fig.11 (b) I_{D1}, V_{ds} for scheme B

As shown in Fig.11(a) and Fig.11(b), the reduction of K_2 makes the converter easier to enter DCM mode but results in a larger current stress for D_1.

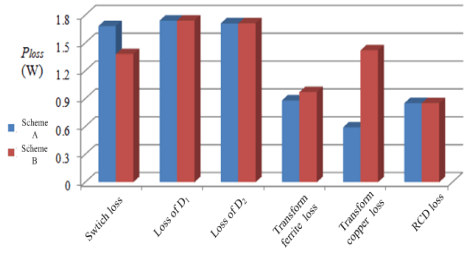

Fig.12 I_{D1}, V_{ds} for scheme A

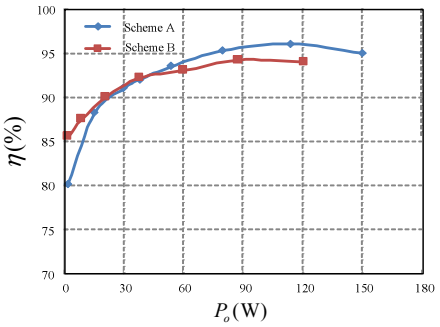

Fig.13 I_{D1}, V_{ds} for scheme B

From Fig.12 and Fig 13, we can know that B has higher efficiency than A, with the highest efficiency of 96% at 120W. However, the decrease of switch frequency increases the RMS

current of the secondary, resulting in more copper loss. Experimental results agree with the analysis very well and testify the proposed converter has the advantage of high efficiency.

V. CONCLUSION

This paper proposes a resonant forward-flyback converter with the concepts of ∑/sigma topology and magnetic integration. The characteristics of the proposed converter are analyzed in detail including the operating principles in different operation modes, the output gain, the ZCS conditions and the power distribution between forward part and flyback part. Besides, this paper also studies the influence of transformer's turns ratios on component stress and power loss. A minimum duty cycle control strategy is proposed to guarantee ZCS of forward diode and valley switching. Finally, a 150 W prototype is constructed to verify the validity of the analysis and the proposed control strategy

REFERENCES

[1] Bo Yang, F. C. Lee, Guisong Huang LLC Resonant Converter for Front End DC/DC Conversion . Applied Power Electronics Conference and Exposition, APEC 2002. Seventeenth Annual IEEE, 2002 : 1108-1112.

[2] M. Khodabakhshian, E. Adib and H. Farzanehfard, "Forward-type resonant bidirectional DC–DC converter," in IET Power Electronics, vol. 9, no. 8, pp. 1753-1760, 6 29 2016.

[3] W. Qin; X. Wu; J. Zhang, "A Current-feed Single-switch Forward Resonant DC Transformer (DCX) with Secondary Diode-clamping," in IEEE Transactions on Industrial Electronics , vol.PP, no.99, pp.1-1

[4] M. Li, Q. Chen, X. Ren, Y. Zhang, K. Jin and B. Chen, "The integrated LLC resonant converter using center-tapped transformer for on-board EV charger," 2015 IEEE Energy Conversion Congress and Exposition (ECCE), Montreal, QC, 2015, pp. 6293-6298.

[5] Xu M, Liu Y, Sun J, et al. Σ/sigma DC/DC conversion for computing and telecom applications[C]// Power Electronics Specialists Conference, 2008. Pesc. IEEE, 2008:1190-1195.

[6] Sun J, Xu M, Reusch D, et al. High efficiency quasi-parallel Voltage Regulators[C]. IEEE. IEEE Xplore, 2008:811-817.

[7] S. De Simone, C. Adragna and C. Spini, "Design guideline for magnetic integration in LLC resonant converters," 2008 International Symposium on Power Electronics, Electrical Drives, Automation and Motion, Ischia, 2008, pp. 950-957

[8] W. Qin; X. Wu; J. Zhang, "A Current-feed Single-switch Forward Resonant DC Transformer (DCX) with Secondary Diode-clamping," in IEEE Transactions on Industrial Electronics, vol.PP, no.99, pp.1-1